Micellization and Gelation of Aqueous Solutions of a Triblock Copolymer Studied by Rheological Techniques and Scanning Calorimetry

ARTICLE *in* THE JOURNAL OF PHYSICAL CHEMISTRY · NOVEMBER 1994

Impact Factor: 2.78 · DOI: 10.1021/j100098a030

4 AUTHORS, INCLUDING:

Karin Schillén
Lund University
80 PUBLICATIONS **2,867** CITATIONS

SEE PROFILE

Micellization and Gelation of Aqueous Solutions of a Triblock Copolymer Studied by Rheological Techniques and Scanning Calorimetry

Søren Hvidt* **and Erling B. Jørgensen**

Department of Chemistry, Roskilde University, DK-4000 Roskilde, Denmark

Wyn Brown and Karin Schillén

Department of Physical Chemistry, University of Uppsala, Box 532, S-751 21 Uppsala, Sweden

Received: February 1, 1994; In Final Form: August 2, 1994[⊗]

The temperature dependent properties of aqueous solutions of a triblock copolymer of ethylene oxide (EO) and propylene oxide (PO), with a measured composition $EO_{28}PO_{48}EO_{28}$, have been investigated by use of rheological techniques and scanning calorimetry at temperatures between 5 and 85 °C and concentrations up to 40 wt %. At low temperatures a unimer−micelle equilibrium is established, which is shown to be due to the interactions between the PO block and water. Complex viscoelastic properties are observed with increasing temperatures. Two sol-to-gel transitions are observed with increasing temperature followed by phase separation. The low-temperature gel, which has a large elastic storage modulus, consists of close-packed spherical micelles. This gel state occurs above a lower critical point of 32 °C and 24.5 wt %. Its large elastic shear modulus is attributed to increasing exposure to water of hydrophobic PO groups in the micellar core under strain. The high-temperature gel, which is formed at concentrations as low as 1−2 wt %, has a smaller elastic modulus which is attributed to hindered rotation of overlapping rodlike micelles. A third gel state, which is a two-phase region, is formed at concentrations above 28%. The complex formation of micelles and gels is summarized in a concentration−temperature diagram.

Introduction

Block copolymers of poly(ethylene oxide) (PEO) and poly(propylene oxide) (PPO) are surface-active reagents with a broad range of technical applications and very remarkable solubility properties.[1] Symmetrical triblock copolymers, with structure $(EO)_x(PO)_y(EO)_x$, where x and y denote the number of EO and PO monomers per block, are often called poloxamers and are commercially available in a range of x and y values. Aqueous solutions of poloxamers have been studied extensively in recent years. Early light-scattering and ultrasound absorption studies showed that aqueous solutions of some of these copolymers contain dissolved unimers at low temperatures but form micelles at higher temperatures.[2−4] It is generally believed that these micelles consist of a core of PPO with a water-swollen mantle of PEO chains.[5] An equilibrium between unimers and micelles of the form

$$n \text{ unimers} \leftrightarrow \text{micelle} \qquad (1)$$

is established, where n is the number of unimers per micelle. The lifetime of a unimer within a micelle has been estimated to be in the microsecond time scale.[6]

Some poloxamers form gels and ordered structures at higher concentrations when heated, and early studies indicated the formation of crystalline cubic structures.[4,7] Recent small-angle neutron-scattering (SANS) studies by Mortensen and co-workers[8−11] have clearly shown that these ordered structures, for a structurally similar copolymer designated as P-85 with a composition $(EO)_{27}(PO)_{39}(EO)_{27}$, are due to close-packing of micelles. Shearing of the gel transfers the system from a polycrystalline state to a long-range-order single cubic crystal.[8,10] Repulsive interactions between spherical micelles were described by use of a Percus Yevick hard sphere potential, characterized by a core radius, R_c, a hard sphere radius, R_{hs}, and a micelle volume fraction, Φ. It was shown that spherical micelles close-pack in the cubic structure when the volume fraction occupied by micelles reaches a critical value of 0.53.[8−11] Both R_c and R_{hs} were found to increase with temperature but were independent of concentration. This shows that n in eq 1 increases with temperature but also that n and the spherical form of the micelles is independent of concentration.[11] At higher temperatures P-85 solutions of higher concentrations also form a hexagonal crystalline phase consisting of rodlike micelles.[11] The transitiion from spherical to rodlike micelles occurs when the diameter of the micellar core becomes comparable to the chain length of the stretched PPO block.[8,10,11] Two other poloxamers, F-87 (x = 62, y = 39) and F-88 (x = 97, y = 39), with the same PO center block but longer EO end blocks, also crystallize in a cubic structure, but a hexagonal phase was not observed, since they form spherical micelles with a smaller core diameter than that of P-85.[9,11]

The gelation process at low temperatures, where cubic packing of spherical micelles is expected, was observed in earlier viscoelastic studies on P-85[12] and on F-87 and F-88.[13] A second sol-to-gel transition at higher temperatures was not resolved in these studies. Recent studies[14,15] show, however, that another copolymer designated as P-94 with the nominal composition $(EO)_{21}(PO)_{47}(EO)_{21}$ undergoes two sol-to-gel transitions. This copolymer has approximately the same nominal molecular weight of 4600 as P-85, but P-94 has a longer PO block which results in more easily detectable lower transition temperatures during both gelation and degelation. Some of the P-94 solution properties have also been characterized by use of a number of other techniques.[14] The main emphasis of the present work was to characterize the temperature dependent viscoelastic properties of P-94 solutions, including the two gellike states. The

* Author to whom correspondence should be addressed at the Department of Chemistry, Roskilde University, DK-4000 Roskilde, Denmark.

⊗ Abstract published in *Advance ACS Abstracts,* October 15, 1994.

0022-3654/94/2098-12320$04.50/0

micellization of P-94 has also been studied by scanning calorimetry, viscosity, and light-scattering techniques, since packing of micelles appears to be directly involved in gelation and crystallization. Micelles of poloxamers are generally thought to involve a core of PPO containing little or no water and a hydrated mantle of PEO. Micellization with increasing temperature is believed to be caused by interactions between water and the PPO block, which is hydrophilic at low temperatues but hydrophobic at higher temperatures.[5] We have therefore studied both a homopolymer of PEO and one of PPO with approximately the same molecular weight as the central block in P-94 in order to investigate this in more detail.

The structures or mechanisms underlying the elasticity of poloxamer gels and the connection between gelation and crystallization are not well understood. It has been variously suggested that the elasticity is related to changes in the PEO mantle,[4] hard sphere interactions between packed micelles,[8] or hydrophobic interactions between the PPO core and water.[7,15] The SANS results indicated a close connection between crystallization and elasticity.[8,11] The hard sphere model predicts that micelles can only occupy a volume fraction of 0.53, and it is therefore unclear what will happen with copolymers present in excess of this concentration. Results presented here suggest that the low- and high-temperature properties of P-94 gels are due to different molecular mechanisms and that the elasticity is dominated by packing and overlapping between micelles rather than by crystallization.

Experimental Section

Materials. The triblock copolymer P-94 was obtained from BASF (Parsippany, NJ). The copolymer was either used as received or purified by extraction of more hydrophobic components with hexane, following a modification of a published method.[16] About 25 g of polymer was extracted three times with 150 mL of hexane at 42 °C in a thermostat with gentle shaking. The hexane phase was decanted off and the remaining polymer dried *in vacuo*. Size exclusion chromatography showed that the unpurified P-94 sample contains about 6% of a lower molecular weight component, which was partly removed by the extraction procedure. A narrow molecular weight PPO with a molecular weight of 2000 was obtained from Waters (Milford, MA), and a PEO sample with a molecular weight of 6000 was obtained from Hoechst (Germany). Both samples were used as received.

The polymer samples in $CDCl_3$ were characterized by ^1H and ^{13}C NMR on a Bruker 250 MHz instrument in order to establish the relative composition of EO and PO, and the molecular weights of the blocks and polymers. The relative composition of EO and PO in the block copolymers was determined from the integral areas under the ^1H resonance peaks (CH_3 at 1.1 ppm, CH_2 and CH at 3.4−3.7 ppm).[16] The number of EO units in PEO-6000 was determined from the ratio of integrals of CH_2 signals from the end groups and from the interior of the PEO blocks in the ^{13}C spectra (resonances at 61.5 and 72.5 ppm for the two C atoms in the terminal EO group; resonances at 70.0−70.4 ppm are CH_2 groups in the interior of the PEO block).[17] The number of PO units in PPO-2000 was obtained from ^{13}C spectra of CH groups (resonance at 65.6−67.3 ppm for the terminal PO group; resonances at 74.7−75.6 ppm are CH groups in the interior of the PPO block).[17] In the case of P-94 the CH_2 resonances at 61.5 and 72.5 ppm are assigned to the two C atoms at the end of the PEO chain; resonances at 68.4 and 70.7 ppm are the two C atoms in the EO unit next to the PPO block; resonances at 70.0−70.4 ppm are the C atoms in the interior of the PEO chains.[17] The composition of P-94, which is shown in Table 1, was then calculated from the number of EO units per block and the ratio of PO and EO. ^1H NMR spectra on unpurified P-94 solutions gave a higher relative PO content of 57.4% compared to that of the purified sample, 53.7%. Hexane extraction removed some components with higher PO content, presumably diblocks or PPO homopolymers. Unpurified and purified P-94 samples showed identical properties in scanning calorimetry and in viscoelastic measurements. Since preliminary light-scattering and cloud point experiments showed effects due to the impurities, all such experiments were therefore subsequently done on purified P-94 samples. Solutions of P-94, PEO, and PPO in distilled water were prepared gravimetrically and allowed to dissolve and mix at 5 °C with gentle shaking overnight. Concentrations reported here are given as weight−weight percent (wt %, grams of polymer per 100 g of solution).

TABLE 1: Characterization of Polymer Samples by NMR and Viscosity

	sample		
property	P-94	PEO-6000	PPO-2000
PO content (%)[a]	53.7		100
EO block length[a]	28	133	
composition[a]	$EO_{28}PO_{48}EO_{28}$	EO_{133}	PO_{37}
M_n (g/mol)[a]	5200	5900	2150
$[\eta]$ (mL/g) at 10 °C	15	19	8
M_v (g/mol)		8200	

[a] From NMR measurements.

Rheological Techniques. Viscoelastic measurements were performed on a Bohlin VOR rheometer (Lund, Sweden) using two stainless steel couette measuring cells C14 (inner diameter 14 mm, outer diameter 15.4 mm, and height 21 mm) and C25 (inner diameter 25 mm, outer diameter 27.5 mm, and height 37.5 mm). The narrow gaps ensure a virtually constant shear through the sample. The outer cylinder is surrounded by a water bath which is connected to a thermostat bath. The temperature was typically varied in steps of 0.5 or 1 °C with 4 min equilibration time at each temperature. Cold polymer solutions were tranferred to the instrument and carefully overlaid with a low-viscosity silicone oil to minimize water evaporation. The instrument measures the temperature in the bath next to the outer cylinder. A temperature correction calibration curve was determined by use of a Grant microthermistor, which was placed in the solution between the inner and outer cylinder in a series of calibration measurements. The correction was significant (up to 4 °C) at extreme temperatures. The VOR instrument was used in the oscillatory mode, where the outer cylinder performs oscillations at a given frequency. The frequency of oscillation was chosen to be 0.05 Hz. The storage and loss shear moduli, G' and G'', are obtained from the time dependence of the stress, σ, by use of the definition[18]

$$\sigma = \gamma_0(G' \sin \omega t + G'' \cos \omega t) \qquad (2)$$

where γ_0 is the strain amplitude and ω is the radian frequency. The strain amplitude can be varied between 0.001 and 0.2 on the instrument, and it was ensured that the measurements reported here were obtained in the linear viscoelastic region, where G' and G'' are independent of the strain amplitude.

A simple falling-ball-type viscometer was used as an independent way to measure gelation and degelation temperatures. It consists of a U-shaped thin-walled glass tube with an inner diameter of 5 mm and a height of 14 cm. Two milliliters of solution and a glass sphere with diameter of 2 mm are transferred to the tube, which is mounted in a small holder and placed in a thermostated bath (±0.1 °C). The holder can be

placed in two positions, which give the vertical parts of the tube an angle of either +30° or −30° with respect to vertical. One side of the tube is closed with a rubber stopper, so the position of the solution is fixed in the tube. The motion of the glass sphere, due to gravity, from one side of the tube toward the other side through the solution, is observed after the tube orientation is changed.

Intrinsic viscosities were determined by use of an Ubbelohde viscometer with a water flow time of 200 s at 20 °C. A 20 min equilibration time was used for each solution in the concentration range 5−50 mg/mL. Intrinsic viscosities were obtained from the common intercepts of the plots of $(t - t_s)/(t_s c)$ and $1/c \ln(t/t_s)$ against c, where t and t_s denote solution and solvent flow times, respectively, and c denotes the concentration of polymer in g/mL.

Differential Scanning Calorimetry. A Perkin Elmer DSC7 scanning calorimeter was used to study the heat capacity of solutions as a function of temperature between 0 and 70 °C. Typically 20−30 mg solutions were placed in aluminum pans, which were then carefully sealed. Thermograms were obtained at rates of 5 °C/min in both heating and cooling scans between −5 and 70 °C, with an empty aluminum pan as reference. The melting point of gallium was used for calibration. The enthalpies of transitions were calculated as the area of the peaks relative to the baseline, which was drawn as a straight line between the baselines prior to and after the transition. Triplicate runs showed that the reproducibility of transition enthalpies for most concentrations was better than ±4%.

Other Techniques. Cloud points were detected by visual inspection of 0.4 mL solutions in sealed thin-walled glass tubes. The tubes were placed in a thermostat bath, and temperatures were increased or decreased in steps of 0.5 or 1 °C with 5 min equilibration time. The temperatures of initial clouding and complete declouding were determined. Static and dynamic light scattering were performed using the instruments and methods described previously.[12,13] The distribution of relaxation time was obtained from Laplace inversion of the intensity correlation functions using the REPES-constrained regularization program. Weight average molecular weights were obtained from static light scattering, as described previously for P-85.[12]

Results

P-94 solutions show dramatic variations in viscoelastic properties as a function of temperature and concentration, as illustrated in Figures 1−3. The viscoelastic properties of 25.5 wt % P-94 and 29.7 wt % PEO-6000 solutions in water are shown in Figure 1 as a function of temperature. The PEO solution has a G'' which far exceeds G' at all temperatures. It is seen that G'' decreases gradually with increasing temperatures. The results for the P-94 solution resemble those for the PEO solution at low temperatures with a similar magnitude of G'' values and a vanishing G'. Several P-94 solutions and the PEO solutions were measured as a function of frequency between 0.001 and 10 Hz at 5 °C. All solutions show $G'' \gg G'$ at all the measured frequencies and that G'' is proportional to the frequency, as expected for a Newtonian liquid, characterized by $G'' = \omega\eta$. With increasing temperature the P-94 solution also initially shows a decreasing G'', but at temperatures about 15 °C, G'' increases with increasing temperature. G' abruptly increases and reaches larger values than G'' at 26 °C. The elastic storage modulus reaches a maximum around 32 °C, where the loss modulus has a minimum value. The frequency dependences of G' and G'' at 32 °C show that G' is much larger than G'' and that G' is virtually independent of frequency between 0.001 and 10 Hz. A plateau in G' is characteristic of a gel state.[19,20] This

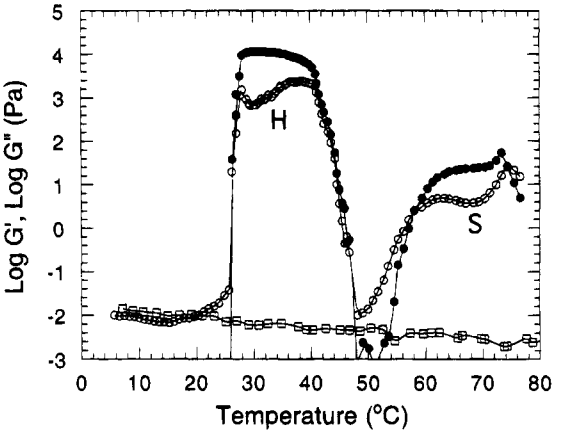

Figure 1. Viscoelastic properties of 25.5 wt % P-94 and 29.7 wt % PEO-6000 solutions as a function of temperature at 0.05 Hz. Symbols are (○) G'' and (●) G' for P-94 and (□) G'' for PEO. H and S mark the hard and soft gels for P-94, respectively.

shows that the solution has changed from a liquid at low temperatures to a gellike state with increasing temperature. The gel point is often[21] estimated as the crossover temperature where $G' = G''$. In a recent definition of the gel point, G' and G'' follow the same power law frequency dependence over a broad range of frequencies, but they are not necessarily equal.[22] Even though the crossover point does not mark the gel point in general, it does mark the temperature where the system changes from a viscoelastic liquid to a viscoelastic solid at the chosen frequency of measurement. The transitions for P-94 solutions occur over such a narrow temperature range that the gel point temperature was estimated as the temperature where $G' = G''$ at the frequency of 0.05 Hz. At temperatures above 40 °C both G' and G'' decrease rapidly. At temperatures between 48 and 58 °C a new viscoelastic liquid is formed, since G'' exceeds G'. Another gel structure is formed at temperatures above 58 °C. This gel will be referred to as the "soft gel" or S, since its elastic modulus is more than 2 orders of magnitude smaller than that of the low-temperature gel, marked H for "hard gel" in Figure 1. The soft gel dissolves again at around 74 °C, and a new viscoelastic liquid state is formed at higher temperatures. The results for the 25.5 wt % P-94 solution show two sol-to-gel transitions and a final gel-to-sol transition, with increasing temperatures. Cooling scans show that all transitions are thermoreversible, with similar moduli in both heating and cooling scans.

The temperature dependent viscoelastic properties are also very dependent on concentration, and the hard and soft gel regions show very different concentration dependences, as illustrated in Figure 2, where G' is plotted against temperature for four solutions with concentrations of 6.3, 24.0, 24.7, and 25.0 wt %. No hard gel is formed at concentrations between 6.3 and 24.0 wt %, whereas a 24.7 wt % solution forms a gel. The critical concentration for formation of this gel is 24.5 ± 0.3%. G' equals G'' for a 24.5 wt % solution (not shown) at 32 °C, whereas G'' exceeds G' at temperatures below and above this temperature. The results in Figures 1 and 2 also illustrate that the temperatures at which the hard gel is formed decrease and temperatures at which the hard gel dissolves increase with increasing concentration above the critical concentration. The soft gel shows much less concentration dependence. Formation of the soft gel is seen at all concentrations down to 1−2 wt %, and the effect of decreasing concentration is only to reduce the plateau G' value and to increase the temperature at which the gel is formed.

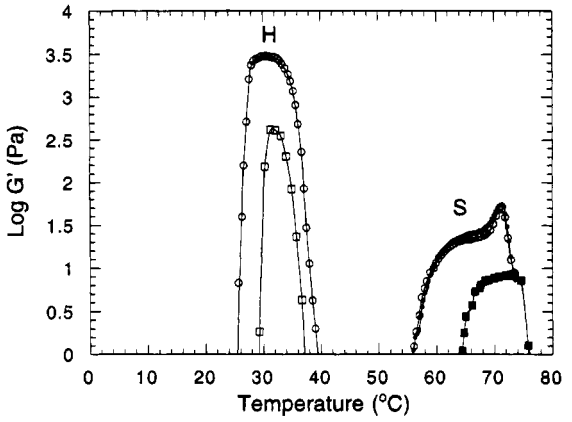

Figure 2. G' for P-94 plotted against temperature at 0.05 Hz for solutions with concentrations in wt %: (■) 6.3; (●) 24.0; (□) 24.7; (○) 25.0. H and S denote hard and soft gels.

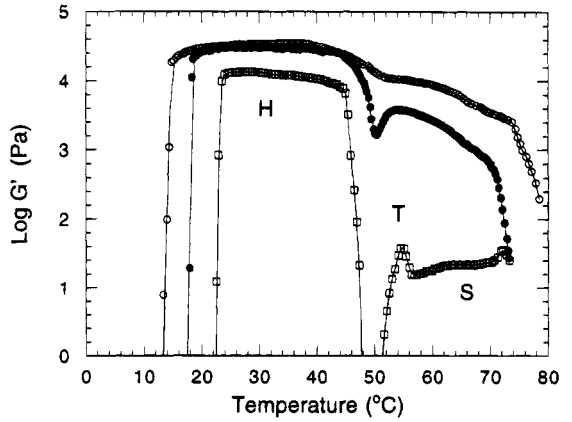

Figure 3. G' for P-94 plotted against temperature at 0.05 Hz for solutions with concentrations in wt %: (□) 27.0; (●) 32.0; (○) 37.0. H and S denote hard and soft gels, and T denotes another gel state (see text).

New viscoelastic effects are also seen at concentrations above 25.5 wt %, as shown in Figure 3 for concentrations of 27.0, 32.0, and 37.0 wt %. A new maximum in G', marked T develops at temperatures between the H and S temperature gel regions. The figure confirms that the temperature region for a stable hard gel increases with temperature and that G' for the H gel increases slowly with increasing concentration. The maximal G' values at all concentrations are near 32 °C. The soft gel seen clearly at lower concentrations in Figures 1 and 2 is perturbed by the new T gel, and only at the lowest concentration of 27 wt % is the plateau clearly seen. G' for all three solutions in Figure 3 decreases rapidly at the highest temperatures, as observed for the lower concentrations in Figures 1 and 2.

The complex viscoelastic properties of P-94 solutions are summarized in Figure 4, which shows a plot of gelation and degelation temperatures, defined as the temperatures where G' equals G'', as a function of concentration. Regions marked L correspond to a liquid or viscoelastic liquid with $G'' > G'$, whereas H and S refer to the temperature regions of the hard and soft gels with $G' > G''$, respectively. The third gel region, marked with a T in Figure 3, is not drawn in Figure 4, since the formation of this type of gel results from a gel-to-gel transition and not a sol-to-gel transition. The concentration dependence of G' for both the hard and soft gels is summarized in Figure 5, which shows G' at 32 °C for the hard gel and G' values at 70 °C in the soft gel plateau at a temperature just below the final gel-to-sol transition temperature. This figure illustrates that G' for the soft gel increases nearly proportionally

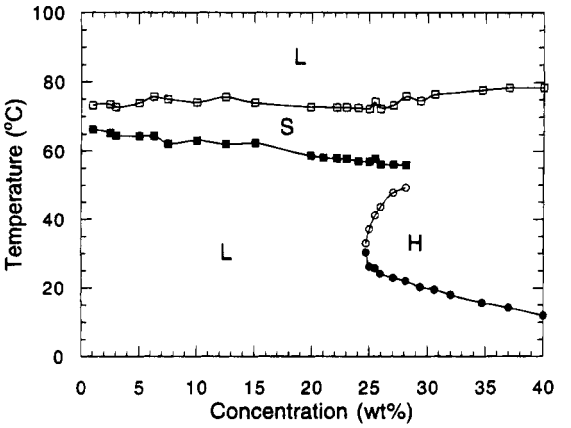

Figure 4. Summary of sol-to-gel transitions at 0.05 Hz for P-94. The plot shows temperatures where G' equals G'' against concentration. L refers to a viscoelastic liquid-like state with $G'' > G'$, and H and S denote gellike states with $G' > G''$. Filled symbols refer to gelation with increasing temperatures; open symbols refer to degelation with increasing temperatures. The reproducibility of onset and degelation temperatures is within ±1 and 2 °C, respectively.

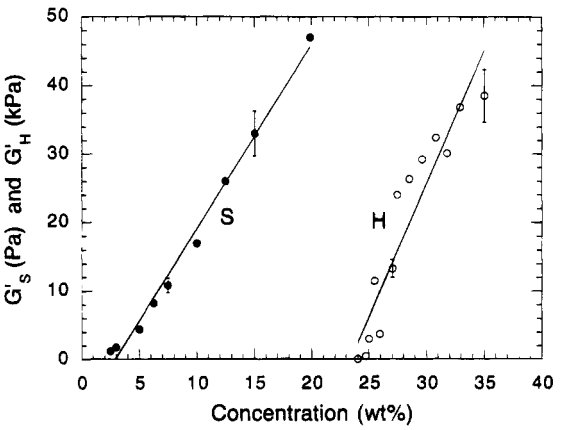

Figure 5. Elastic storage modulus, G', at 0.05 Hz for P-94 solutions plotted against concentration at 32 °C for hard gel (○) and at 70 °C for soft gel (●). The uncertainties of the G'_S and G'_H values marked with bars are ±10% of their values.

to concentration. The hard gel shows a roughly linear increase in G' with concentration above the critical gelation concentration.

The degelation temperatures of the hard gel are difficult to determine precisely from the viscoelastic data, since G' and G'' are almost equal over a fairly broad temperature range. In order to get an independent estimate of gelation and degelation temperatures, solutions were also studied by monitoring the motion of a glass sphere in tubes with P-94 solution. The gel points were taken as the first temperature where no detectable motion of the sphere due to gravity was noticeable in a period of 3 min. Degelation temperatures were similarly taken as the temperature where the sphere started to move. Similar gelation and degelation temperatures were observed when solutions were cooled and heated. Results obtained in a broad concentration range are summarized in Figure 6. The observed degelation temperatures for the soft gel are omitted for clarity reasons, but the temperatures showed a gradual increase from 76 to 82 °C between 1 and 40 wt %. The gelation and degelation temperatures obtained from the viscoelastic measurements in Figure 4 are traced as curves in Figure 6 for comparison. It is seen that both methods detect the hard and soft gel and that the agreement is perfect for the hard gel region. The onset of the soft gel occurs at about 5 °C higher temperatures when determined by the falling-sphere method. This is probably due to the fact that

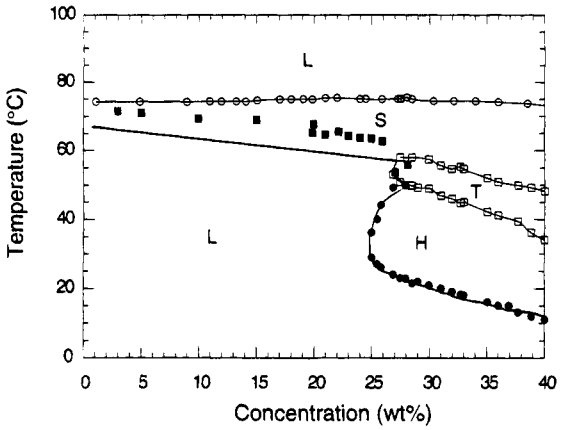

Figure 6. Gelation and two-phase regions for P-94 solutions. Filled symbols refer to temperatures where glass spheres become unable to move. Heavy curves are traces of gelation curves from viscoelastic measurements in Figure 4. Open symbols and fine curves denote temperatures where a transition between two phases and a single phase is observed. H, S, and T refer to hard gel, soft gel, and two-phase gel, respectively. L is a liquid state.

the falling-ball method determines the yield stress, which is expected to be very low near the gel point for the soft gel, since G' values are small.

It was noticed that solutions became cloudy in certain temperature regions during some of the viscoelastic runs. This indicates the existence of two-phase regions. Purified P-94 solutions with concentrations between 1 and 40 wt % were heated in thin-walled tubes and inspected visually in order to investigate this further. The temperatures where solutions were first visually detected to become cloudy were determined together with similarly determined declouding temperatures. The temperatures were reproducible to within 1 °C, and good agreement was obtained in both heating and cooling experiments. The temperatures are summarized in Figure 6, which shows that at concentrations below 27 wt % solutions are homogeneous at temperatures between 0 and approximately 74 °C. Above this temperature solutions are cloudy up to 100 °C. Solutions with concentrations between 28 and 40 wt % are also cloudy between 74 and 100 °C, but in addition these solutions also exhibit a cloudy two-phase region at lower temperatures. It is seen that both clouding and declouding temperatures decrease with increasing concentration for this two-phase region. The concentration range and clouding temperatures closely correspond to conditions where the gel state, denoted T in Figure 3, is seen. The cloud point determinations therefore show that the T gel is a two-phase gel.

Six solutions of purified P-94 with concentrations between 0.01 and 0.1 g/mL were studied by static light scattering as a function of temperature between 10 and 50 °C, as described previously for P-85.[12] No angular dependence was observed, as expected for these small particles. Weight average molecular weights were obtained by an extrapolation of Kc/R to vanishing concentrations. The extrapolated intercept at low temperatures was uncertain, due to a low scattering intensity and a significant concentration dependence. The molecular weights obtained at 10, 15, and 20 °C were around 4000 g/mol, which is somewhat smaller than the unimer molecular weights given in Table 1. It is on the limit of the light-scattering method to make precise measurements on a polymer of such low M_w. The scattered intensity is too low and only slightly above the intensity of the solvent. Error bars of the magnitude 50% would be acceptable in this M_w range. Within the limits of experimental uncertainty, the M_w represents the monomeric species. The scattered intensity increases with increasing temperature and at 40 and

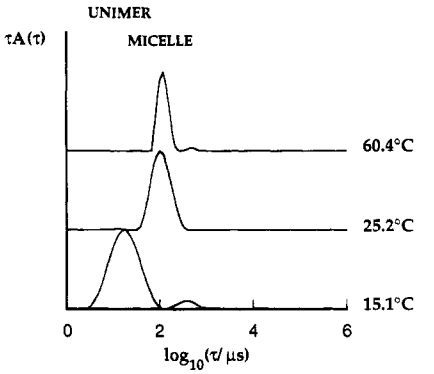

Figure 7. Normalized distribution of relaxation times, τ, calculated from dynamic light scattering at a 90° scattering angle on a 5.0 wt % purified P-94 solution at the temperatures indicated on the figure. Peaks attributed to unimers and micelles are indicated.

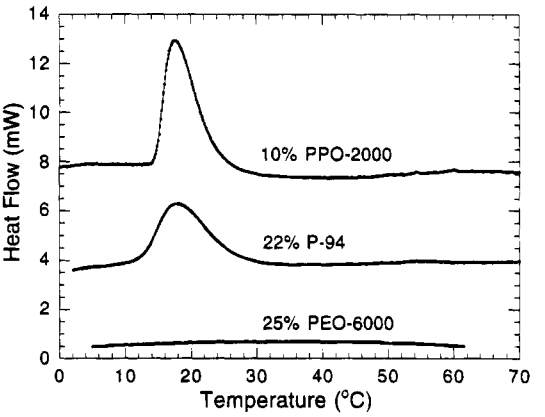

Figure 8. Scanning calorimetry at 5 °C/min for PPO-2000, P-94, and PEO-6000 solutions. Heat flow is plotted against temperature. The enthalpies of the endothermic transitions are obtained from the area under peaks.

50 °C resulted in molecular weights of 190 and 320 kg/mol. These molecular weights and a P-94 unimer molecular weight of 5200 g/mol correspond to micellar aggregation numbers of 37 and 62 at 40 and 50 °C, respectively.

Dynamic light-scattering experiments were performed on 5% solutions of both purified and unpurified P-94 solutions. The distribution of relaxation times for the unpurified solutions at low temperatures is similar to earlier results obtained on unpurified P-85 solutions showing a broad and complex distribution of relaxation times. The relaxation time distributions for the purified solution at 15.1, 25.2, and 60.4 °C are shown in Figure 7. This figure illustrates that purification of P-94 results in a fairly simple distribution of relaxation times at 15.1 °C with a dominating peak, which from the apparent hydrodynamic radius can be assigned to fast diffusing single copolymer molecules. It is also seen that the purification procedure has not completely removed slower diffusing components, which are attributed to small concentrations of clusters due to remaining contaminants. The figure illustrates that a transition from unimers to micelles, with a correspondingly longer relaxation time, occurs between 15 and 25 °C. A low-amplitude slow component is also seen when the temperature is raised to 60 °C. The apparent hydrodynamic radii at $c = 5$ wt % were calculated from the measured diffusion constants of the main peak by use of the Stokes–Einstein relation and were 14, 84, and 99 Å at 15, 25, and 60 °C, respectively.

To further investigate the mechanism of micellization, differential scanning calorimetry (DSC) was employed. Figure 8 shows a plot of heat flow as a function of temperature for a 22 wt % P-94 solution. The heat capacity is given by the heat

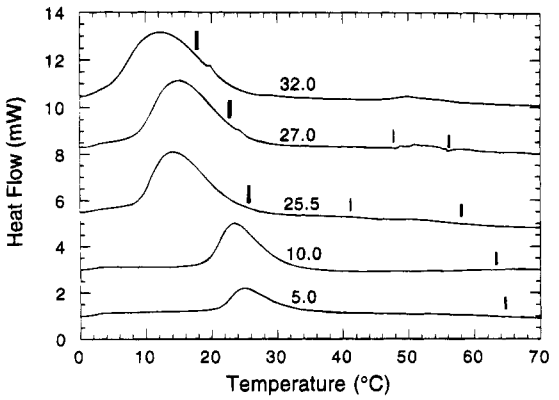

Figure 9. Scanning calorimetry on P-94 solutions at the concentrations (in wt %) indicated on the thermograms. Heavy bars indicate gelation, and fine bars degelation temperatures from the viscoelastic measurements in Figure 4.

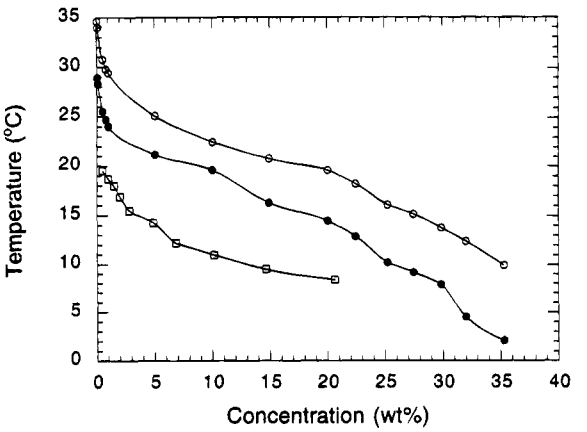

Figure 10. Plots from scanning calorimetry of temperatures for onset of micellization (●) and peak heat capacity (○) plotted against concentration for P-94 solutions. Plot of clouding temperature for PPO-2000 (□) against concentration.

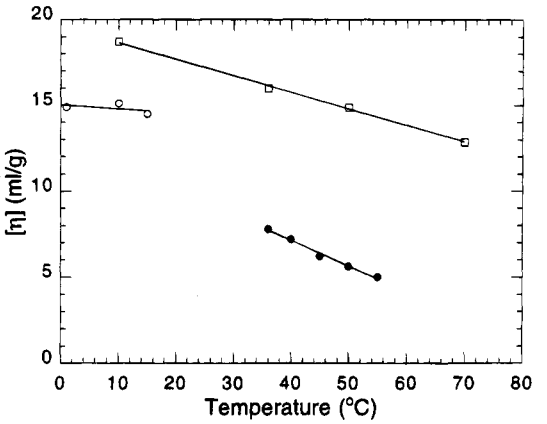

Figure 11. Plot of intrinsic viscosity against temperature for P-94 as unimers (○), P-94 as micelles (●), and PEO-6000 (□).

flow times the scan rate, which in these experiments was 5 °C/min. An endothermic transition with a fairly long tail on the high-temperature side is seen for the P-94 solution. The transitions were characterized by two temperatures, T_p and T_{on}, which denote the temperature of maximum heat capacity and the onset of transition, respectively. The 25 wt % solution of PEO-6000 does not show any sign of a cooperative transition between 5 and 60 °C. However, a 10 wt % solution of PPO-2000, which roughly corresponds to the central block in P-94, undergoes an endothermic transition with an onset temperature very close to the onset temperature for P-94. The good agreement between the two peaks and the lack of a transition for PEO demonstrate that it is the PPO part of P-94 which undergoes a transition during micellization, whereas the PEO part does not contribute to the transition but prevents the P-94 from forming a two-phase state by keeping the PPO in solution as micelles. A more detailed analysis of the shape of the endothermic peaks will be given elsewhere.[23]

The onset temperature of micellization decreases with increasing concentration, as seen in Figure 9. The onset of the endothermic transition for the 5% solution is at 21 °C, and the transition extends to about 40 °C. The dynamic light-scattering results in Figure 7 at the same concentration showed unimers at 15 °C and an almost complete transition to micelles at 25 °C. The calorimetry results, on the other hand, show that only about half of the P-94 is in the micellar form at 25 °C. This apparent difference is due to the fact that the scattering intensity is heavily weighted to the higher molecular weight micelles. The specific enthalpies of micellization determined from the areas under the transition were independent of concentration between 5 and 37.5 wt % and were 50 ± 4 J/g of P-94. Enthalpies for PPO-2000 were obtained for solutions with concentrations between 3 and 20 wt %. The enthalpy was 105 ± 4 J/g of PPO. When the measured enthalpy of P-94 is expressed as J/g of PPO, a value of 97 J/g is obtained. This value is in very good agreement with the value determined for PPO-2000, and the slightly lower value for P-94 may be ascribed to exposed PO groups at the surface of the core of the micelles. Cooling scans on P-94 and PPO solutions (not shown) showed that the transitions are reversible with the same enthalpies and a small (about 2 °C) hysteresis. The bars in Figure 9 refer to temperatures of gelation for both hard and soft gels from Figure 4. It is seen that the formation of the soft gel does not give rise to any detectable endothermic transition. The formation of the hard gel for the 25.5% solution, which was illustrated in Figure 1, does not give rise to any detectable transition, whereas very small peaks are detected at temperatures close to onset of gelation at the two higher concentrations. The three high-concentration scans also show that the peak extends at temperatures above the onset of gelation. This shows that additional unimers also undergo transitions at temperatures above the gelation point.

Figure 10 shows the concentration dependence of the onset temperature and the temperature corresponding to the maximum heat capacity. Data for cloud points of PPO-2000 solutions are also shown. It is seen that the onset of micellization for P-94 roughly corresponds to the cloud point of the PPO-2000, recalling that only half of the P-94 is PPO. The tail of the thermogram for the 5 wt % solution of P-94 in Figure 9 was used to estimate the concentration of unimers at higher temperatures. The concentration of free unimers at a given temperature was obtained from the fraction of the endothermic transition remaining at that temperature. The free unimer concentration at 32 °C was estimated to be less than 0.1%.

Micellization of P-94 is expected to involve the formation of more compact structures. This was investigated by capillary viscosity measurements at selected temperatures. Figure 11 shows that the intrinsic viscosity of P-94 is around 15 mL/g at temperatures between 1 and 15 °C, where unimers are expected from scanning calorimetry and light scattering. Intrinsic viscosities were not determined at intermediate temperatures where the unimer−micelle equilibrium dominates. The intrinsic viscosity of micelles was determined at higher temperatures, at which the concentration of unimers is very small (<0.1%). Figure 11 shows that micellization results in a drop in intrinsic viscosity and that the intrinsic viscosity of the micelles decreases

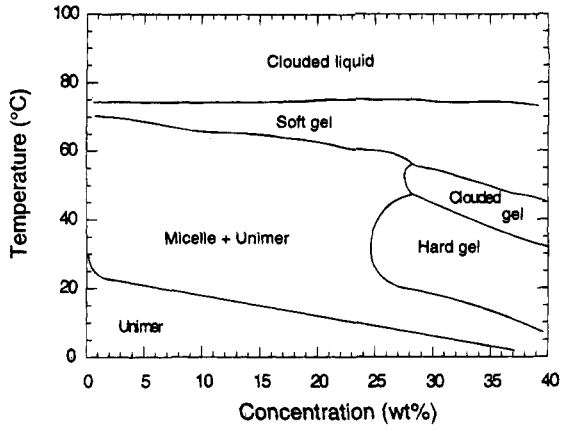

Figure 12. Diagram showing the combined concentration and temperature conditions where P-94 is found as unimers, micelles, and gels in water, as determined by use of viscoelastic, scanning calorimetry, and cloud point techniques.

with temperature between 36 and 55 °C. A least squares linear fit to the data in this temperature range gives

$$[\eta]/\text{mL g}^{-1} = (13.1-0.15T) \qquad (3)$$

where T is the temperature in °C. The static light-scattering results showed that the number of unimers per micelle increases over the same temperature as discussed above. The two results combined show that the micelles become more compact per mass of copolymer but an increase occurs in the number of unimers per micelle. Figure 11 also shows the intrinsic viscosity of PEO-6000 as a function of temperature. It is seen that the intrinsic viscosity decreases with increasing temperature. This suggests that the decrease in intrinsic viscosity of P-94 with temperature is due to both an increase in micellar aggregation number and to contraction of the PEO arms of the P-94 micelles.

Discussion

The properties of aqueous solutions of P-94 are shown to be very dependent on temperature and concentration. The viscoelastic results demonstrate that P-94 solutions can undergo complex sol-to-gel transitions. At concentrations above 24.5 wt % a gel state is formed with a critical temperature of 32 °C at 24.5 wt %. This gel state is denoted the "hard gel" since the elastic moduli are very high, between 1−4 10^4 Pa, which is only 1−2 orders of magnitude lower than those for typical cross-linked undiluted rubber networks.[18] At concentrations between 24.5 and 28 wt % this gel dissolves again at higher temperatures and a low modulus viscoelastic liquid is formed. Earlier viscoelastic studies[12,13] on P-85, F-87, and F-88 showed the formation of similar hard gels and also showed that the onset temperatures of gelation decreased with increasing concentration. The higher temperature "soft gel" for P-94 with moduli between 1 and 50 Pa and the two-phase gel region were not detected in the earlier viscoelastic studies. The soft gel region is terminated at high temperatures by a two-phase liquid state, with a cloud temperature which is virtually independent of concentration. At concentrations above 28 wt % another gel state is observed. This gel state consists of two phases, and it separates the hard and soft gel regions. It may consist of a mixture of hard and soft gels. The elastic storage modulus gradually decreases with temperature through this two-phase region.

The combined results from viscoelastic, scanning calorimetry, and clouding experiments are summarized in Figure 12, which shows the temperature and concentration regions where unimers, micelles, and the different gel forms are observed. At low temperatures the light-scattering and intrinsic viscosity results show that solutions consist of dissolved unimers. Micelles are formed when the temperature is increased. The onset temperature of micellization decreases with increasing concentration, as seen by the scanning calorimetry results. Figure 12 shows many similarities and some interesting differences compared to a structural phase diagram for P-85 based on SANS[10] and light-scattering results.[12] Both studies show that unimers are present at low temperatures and that a unimer−micelle equilibrium is formed with increasing temperature. A linear dependence of the critical micellar concentration on temperature was found for P-85, and except at lower concentrations, a more or less linear dependence is also seen for P-94. The hard gel region for P-94 occurs at concentrations and temperatures quite similar to a cubic crystalline region observed for P-85, although the boundaries are apparently of a somewhat different shape. The soft gel region at higher temperatures for P-94 corresponds to temperatures where a hexagonal crystalline region was observed by SANS on P-85, except that the soft gel is seen for P-94 at concentrations as low as 1−2 wt %, whereas the crystalline region for P-85 is limited to concentrations above about 14 wt %. A liquid channel seen in P-85 using SANS and lying between the cubic and hexagonal structures between 20 and 40 wt % is only seen between 24.5 and 28 wt % in the viscoelastic results on P-94. Both the viscoelastic and the falling-ball results demonstrate the absence of a liquid channel at concentrations between 28 and 40 wt %.

The DSC results are consistent with the often assumed model for the micelle with a core of PPO and a mantle of PEO chains. The light-scattering and viscosity results show that the micelles increase in mass but decrease in specific volume with increasing temperature. This is consistent with the intrinsic viscosity data on PEO, which shows that the PEO coils become less expanded as water becomes a poorer solvent for PEO. The viscosity average molecular weight, M_v, is calculated to be 8600 g/mol from the Mark−Houwink type relationship, $[\eta]/\text{mL g}^{-1} = 2 + 0.016M_v^{0.76}$ at 20 °C from ref 24 and the interpolated value of 17.7 mL/g from Figure 11. Under Θ conditions a 8600 g/mol PEO has an intrinsic viscosity[24] of 10−12 mL/g. Figure 11 shows therefore that water is a good solvent for the PEO in the entire temperature region investigated in our study.

If micelles are modeled as hard spheres, the Einstein relation connects the intrinsic viscosity to the volume fraction, Φ_v, and the equivalent hard sphere radius, R_v, through

$$[\eta] = 2.5\Phi_v/c = (10\pi/3)(N_a/M)R_v^3 \qquad (4)$$

where N_a is Avogadro's number, c the copolymer concentration (in g/mL), and M the molar mass of micelles. When the temperature dependent intrinsic viscosity of the micelles from eq 3 is introduced, the hard sphere micelle volume depends on weight concentration of micelles, c, and temperature, T, as

$$\Phi_v = (c/2.5)(13.1 - 0.15T) \qquad (5)$$

At the critical gelation point (24.5 wt % and 32 °C), where Figure 10 shows that the unimer concentration is negligible (0.1 wt %), Φ_v is then 0.81. This value is significantly higher than the theoretical value of 0.53 expected for a cubic-packing of hard spheres.[8] The calculated volume fraction suggests that the PEO chains in the mantle overlap considerably or are compressed in the gel state. Additional support for this view is seen from the viscoelastic measurements, which clearly show that the elastic modulus continues to increase both with increasing temperature above the gelation temperature and when

a higher polymer concentration is used above the critical concentration of 24.5 wt % for gelation (see Figures 1−5). The DSC results also show that micellization continues above the gelation temperature (see Figure 10). These results show that the gel with packed micelles can accommodate more copolymer past the gelation point. Since it seems clear from the SANS data that the core radius depends on temperature but not on concentration, the conclusion is that the number of micelles increases. The onset of the two-phase gel may indicate the maximum packing which the gel can accommodate. At 32 °C the onset concentration for two-phase formation is about 42 wt %, as seen from Figure 6. This corresponds, by use of eq 5, to an equivalent apparent hard sphere volume fraction of 1.39. The hard gel can therefore accommodate nearly 70% more polymer than necessary for gelation. This argues against a simple hard sphere potential with a concentration independent hard sphere radius but is not in opposition to the presence of strong repulsive interactions between micelles which may result in crystallization.

The shape of the hard gel region in Figure 12 may qualitatively be explained as due to two opposing effects: (i) more micelles are formed with increasing temperatures, and (ii) the specific volume of the micelles decreases with increasing temperature. Following this idea the critical point is identified as the concentration and temperature at which the volume increase from additional micelles is compensated by the decrease in the specific volume of the micelles. The gelation temperature for the highest concentration studied (40 wt %) is 12 °C, and at this temperature the micellar weight concentration is approximately 20 wt %, as seen from Figure 10. The intrinsic viscosity for micelles at 12 °C is about 11 mL/g, as estimated from eq 3. The onset of gelation therefore corresponds to a Φ_v value of 0.88, in reasonable agreement with the Φ_v value of 0.81 at the critical point. The onset of gelation is therefore determined by the concentrations and temperatures at which Φ_v has a critical value of about 0.85. Above the critical temperature the additional unimers added to micelle cannot compensate for the drop in intrinsic viscosity and micellar volume, and the gel dissolves when the volume fraction of the micelles is less than the critical volume fraction.

It is unclear whether the gel regions consist of crystals of micelles, which can be formed by shearing of samples.[8] The scanning calorimetry data do not detect any endothermic transitions corresponding to temperatures at which soft gels are formed. It is unclear whether the hard gel formation necessarily involves formation of an ordered cubic lattice. In some cases a small peak appears at temperatures close to the gelation temperature, as shown in Figure 9, but it is not established if these peaks are due to crystallization or merely a small extramicellar formation. Our results and other studies[25,26] show that any crystallization transition involves at most a few percent of the enthalpies involved in micellization. The experimental observation that degelation does not result in exothermic peaks suggests that our samples are not crystalline but rather consist of amorphous closed-packed spheres. The observation that the formation of the soft gel is a gradual process with temperature and concentration also argues against crystallization as the cause of gelation. Furthermore, hexagonal crystals of P-85 were only observed down to concentrations of about 14 wt % whereas the gel state extends down to 1−2%. We attribute the soft gel formation to an overlapping of rodlike micelles, since theoretical calculations[27] on several poloxamers predict a transition from spherical to rodlike micelles with increasing temperature and since studies on P-85, which has close structural similarities, have shown that spherical micelles become increasingly asymmetric and rodlike with increasing length at temperatures approaching the cloud point.[11] Following this idea, the gelation temperature can be interpreted as the temperature where the length of the rodlike micelles is sufficient to give relaxation times on the order of seconds due to hindered rotation by the overlapping of micellar rods. A longer length, which necessitates a higher temperature, is needed at a lower concentration of polymer to form semidilute solutions of overlapping rods.

The molecular mechanisms or structures responsible for the elastic moduli are not understood. The work presented here and results from other studies demonstrate the importance of the concentration of micelles, and it is clear that the hard gel consists of close-packed micelles which may or may not form a cubic crystal. The present results suggest that the PEO mantles overlap considerably, and one possibility is that the elastic modulus is due to entangling of PEO chains anchored on different micelles. However, the molecular weight of the PEO blocks is only 1200, which is much too low to give rise to a plateau zone in any polymer solution.[18] The viscoelastic data for PEO in Figure 1 at a much higher concentration and molecular weight demonstrate that PEO chains by themselves cannot give an elastic contribution on the time scale of seconds or longer. The PPO core of the poloxamer micelles is in a liquid-like state, as is seen from a range of diffusion measurements and NMR,[14,28] so it is not likely that the elastic modulus is due to the liquid core of the micelles. These considerations show that both the PEO mantle and the PPO core are in the liquid state and thus cannot give rise to the large elastic moduli. We have recently proposed[15] that the elasticity is due to interactions between the PPO surface of the micellar core and water. If PEO chains anchor micelles in a close-packed situation and if the deformation of the entire gel is affine, then the surface area of the core will increase during a shear deformation. The elasticity is then determined by the additional area created by the deformation and the interfacial tension, Γ, between water and PPO. On the basis of these assumptions, the elastic modulus can be expressed by[15]

$$G' = N\Gamma 4\pi R^2({}^4/_{15} - {}^{12}/_{105}\gamma^2 + O(\gamma^4)) \qquad (6)$$

where N is the number density of micelles and R is the radius of the micellar core. The static light-scattering results show that each micelle contains 37 unimers (and PPO blocks) at 40 °C, which corresponds to an R value of 3.4 nm on the basis of a PPO density of 1.01 g/cm^3.[10] The interfacial tension has been estimated by Wanka and co-workers[7] to be approximately 1 mJ/m^2. For a 30 wt % P-94 solution we can therefore estimate N to be 9.4×10^{23} m^{-3} and G' to be about 36 kPa at small strains. The measured G' values are typically 10−40 kPa, as seen in Figure 5. The measured values are seen to be slightly smaller than the theoretical value. However, the latter figure is based on the assumption that the entire PPO core surface is in contact with water. This is clearly an overestimate of the PPO water contact area, since this ignores the area occupied by the PEO chains which connect the core and the mantle. Equation 6 predicts a linear concentration dependence of G'. The experimental data in Figure 5 show a similar concentration dependence, despite considerable scatter.

The elasticity of the soft gel, which as discussed above contains overlapping rodlike micelles, may be due to the interactions between water and the cylindrical PPO core. Shear deformation of a long rodlike structure should result in a much smaller increase in surface area, but a rigorous calculation has not been performed. Another possibility is that the elasticity is merely due to hindered rotation of overlapping rods. At frequencies higher than the frequency of the hindered rotation of rods, G' for overlapping rods becomes[24]

$$G' = {}^3/_5 \nu RT \quad (7)$$

where ν is the molar concentration of rods. This equation predicts a linear dependence of G' on concentration, which is in agreement with the results in Figure 5. An estimate of the expected modulus can be made on the basis of the recent determination of the length of P-85 rodlike micelles.[11] From depolarized light scattering, a length and core radius of about 160 and 6 nm were determined, corresponding to about 4700 unimers per micelle. Assuming similar dimensions for P-94, a 10 wt % solution therefore has a ν value of 4×10^{-3} mol/m^3, which at 70 °C corresponds to a shear modulus of 7 Pa of similar magnitude to the measured value in Figure 5. The critical concentration where rods of length L start to overlap is given by a number density equal to $1/L^3$.[29] With the above rod length and diameter, the critical concentration for overlapping rods is 1.0 wt %, which is close to the lowest concentration where the soft gel was observed.

Conclusions

The P-94 polymers dissolve as unimers at low temperatures but form micelles with increasing temperatures due to hydrophobic interactions between the PPO block and water. At higher concentrations the micelles overlap considerably and form a hard gel consisting of close-packed spherical micelles. The elasticity of this gel is due to exposure of the PPO core to water with strain. The gel, which may or may not be crystalline, can accommodate a high concentration of micelles, and even though the micelles presumably repel each other, no signs of a concentration independent hard core potential is seen. A softer gel which is detected at higher temperatures is formed down to very low concentrations, and its elasticity is consistent with hindered rotation of overlapping rods rather than crystallization.

Acknowledgment. Valuable discussions with Kell Mortensen (Risø) and Mats Almgren (Uppsala) are greatly appreciated. We thank Christina Fog Hansen and the late Ester Hellgren for expert technical assistance, and A. Hvidt is thanked for access to the scanning calorimeter. Financial support from the Danish Research Council (S.H.) and the Swedish Natural Science Council (W.B.) is gratefully acknowledged.

References and Notes

(1) Lundsted, L. G.; Schmolka, I. R. In *Block and Graft Copolymerization*; Ceresa, R. J., Ed.; Wiley: New York, 1976; pp 1–111.
(2) Zhou, Z.; Chu, B. *Macromolecules* **1987**, *20*, 3089–3091.
(3) Zhou, Z.; Chu, B. *J. Colloid Interface Sci.* **1988**, *126*, 171–180.
(4) Rassing, J.; Attwood, D. *Int. J. Pharm.* **1983**, *13*, 47–55.
(5) Schick, M. J. *Nonionic Surfactants. Physical Chemistry*; Marcel Dekker: New York, 1987.
(6) Fleischer, G. *J. Phys. Chem.* **1993**, *97*, 517–521.
(7) Wanka, G.; Hoffmann, H.; Ulbricht, W. *Colloid Polym. Sci.* **1990**, *268*, 101–117.
(8) Mortensen, K. *Europhys. Lett.* **1992**, *19*, 599–604.
(9) Mortensen, K.; Brown, W.; Nordén, B. *Phys. Rev. Lett.* **1992**, *68*, 2340–2343.
(10) Mortensen, K.; Pedersen, J. S. *Macromolecules* **1993**, *26*, 805–812.
(11) (a) Mortensen, K.; Brown, W. *Macromolecules* **1993**, *26*, 4128–4136. (b) Schillén, K.; Brown, W.; Johnson, R. M. *Macromolecules* **1994**, *27*, 4825–4832.
(12) Brown, W.; Schillén, K.; Almgren, M.; Hvidt, S.; Bahadur, P. *J. Phys. Chem.* **1991**, *95*, 1850–1858.
(13) Brown, W.; Schillén, K.; Hvidt, S. *J. Phys. Chem.* **1992**, *96*, 6038–6044.
(14) Bahadur, P.; Pandya, K. *Langmuir* **1992**, *8*, 2666–2670.
(15) Jørgensen, E. B.; Jensen, J. H.; Hvidt, S. *J. Non-Cryst. Solids* **1994**, *172–174*, 972–977.
(16) Reddy, N. K.; Fordham, P. J.; Attwood, D.; Booth, C. *J. Chem. Soc., Faraday Trans.* **1990**, *86*, 1569–1572.
(17) Heatley, F.; Luo, Y.-Z.; Ding, J.-F.; Mobbs, R. H.; Booth, C. *Macromolecules* **1988**, *21*, 2713–2721.
(18) Ferry, J. D. *Viscoelastic Properties of Polymers*, 3rd ed.; Wiley: New York, 1989.
(19) Clark, A. H.; Ross-Murphy, S. B. *Adv. Polym. Sci.* **1987**, *83*, 57–192.
(20) Almdal, K.; Dyre, J.; Hvidt, S.; Kramer, O. *Polym. Gels Networks* **1993**, *1*, 5–17.
(21) Tung, C. Y. M.; Dynes, P. J. *J. Appl. Polym. Sci.* **1982**, *27*, 569–574.
(22) (a) Winter, H. H.; Chambon, F. *J. Rheol.* **1986**, *30*, 367–382. (b) Chambon, F.; Winter, H. H. *J. Rheol.* **1987**, *31*, 683–697.
(23) Lopez-Lacomba, J. L.; Hvidt, S. In preparation.
(24) Brandrup, J.; Immergut, E. H. *Polymer Handbook*, 3rd ed.; Wiley: New York, 1989.
(25) Vadnere, M.; Amidon, G.; Lindenbaum, S.; Haslam, J. L. *Int. J. Pharm.* **1984**, *22*, 207–218.
(26) Deng, Y.; Yu, G.-E.; Price, C.; Booth, C. *J. Chem. Soc., Faraday Trans.* **1992**, *88*, 1441–1446.
(27) Linse, P. *J. Phys. Chem.* **1993**, *97*, 13896–13902.
(28) Almgren, M.; Bahadur, P.; Jansson, M.; Li, P.; Brown, W.; Bahadur, A. *J. Colloid Interface Sci.* **1992**, *151*, 157–165.
(29) Doi, M.; Edwards, S. F. *The Theory of Polymer Dynamics*; Oxford University Press: Oxford, U.K., 1986; Chapter 9.